Excerpt from the Proceedings of the 2011 COMSOL Conference in Boston

Study of AC Electrothermal Fluid Flow Models

Sophie Loire[*,1], Paul Kauffmann[1] and Igor Mezić[1]
[1] Department of Mechanical Engineering, University of California, Santa Barbara, CA, 93106
*Corresponding author: sloire@engr.ucsb.edu

Abstract: Driving fluid flows with an electric field has promising applications for mixing, concentration, pumping application in lab on chip. However current models are still inaccurate and don't fit the measures. This work is focused on AC electrothermal fluid flow. The simple decoupled model presented by Ramos *et al.* doesn't fit correctly the measured AC electrothermal fluid flows at high temperature gradient. We perform an in-depth theoretical analysis of the multiphysics couplings for electrothermal flows. Numerical simulations performed with COMSOL multiphysics using strongly coupled equations are compared to experimental results. The model for high temperature gradient presented here matches more accurately the datas.

Keywords: Multiphysics, microfluidic, joule heating, electrothermal.

1. Introduction

Labs on a chip are a tool developed for pharmaceutical applications to perform laboratory operations on a small scale, using miniaturized devices. Driven by their portability and affordability advantage, new applications in environmental monitoring or medical diagnostics are now also developed. In such autonomous devices, manipulation of media requires fully integrated actuators. One promising way to generate flows is based on AC electrokinetic, which is driven by the interaction between a electric field and a polarizable and/or conductive solution. Various phenomena generated by AC electrokinetic have been characterized: AC Electro-osmosis (ACEO), AC electrothermal (ACET) and buoyancy (BF) [1]. For most electrode and channel designs, these flows appear in the form of vortices which can be used for diverse purposes e.g. mixing, pumping, etc [2]… For the past ten years, some differences between experimental flows especially at high temperature gradient and ACET models have been observed [3]. This paper proposes a new model implemented with COMSOL to take into account high temperature gradient. After a short reminder of the theory of ACET, we explain the small temperature gradient assumption that ACET models typically use. Then our high temperature gradient model is detailed. This is followed by the description of the COMSOL Multiphysics implementation. Theoretical and experimental results are finally compared.

1.1 AC Electrothermal Fluid Flow

Electrothermal flow is a well-known phenomenon, which arises in systems with non-uniform permittivity and conductivity. In such a system, a local free charge distribution is present. The local charge density responds to the applied electric field resulting to a non zero volume force on the fluid. The electrostatic force density acting on an aqueous solution in the presence of an electric field is given by:

$$\boldsymbol{F}_{ET} = \rho_e \boldsymbol{E} - \frac{1}{2}|\boldsymbol{E}^2|\boldsymbol{\nabla}\varepsilon_m \qquad (1)$$

where ρ_e is the local charge density, $\boldsymbol{E}$ the electric field and ε_m is the solution permittivity.

ACET fluid flow arises from the interaction of the external electric field with temperature-induced inhomogeneities in medium conductivity and permittivity due to Joule heating. The temperature distribution is given by a time averaged Joule heating equation:

$$\boldsymbol{\nabla}.(k_m(T)\boldsymbol{\nabla}T) + \frac{\sigma_m}{2}|\boldsymbol{E}|^2 = 0 \qquad (2)$$

where k_m is the fluid heat conductivity, σ_m is the fluid conductivity, T is the temperature and $\boldsymbol{E}$ is the complex representation of the electric field.

The resulting local charge density can be estimated by the usual Maxwell-Wagner-type charge balance between Coulomb and dielectric forces:

$$\rho_e = \boldsymbol{\epsilon}_m\left(\frac{1}{\boldsymbol{\epsilon}_m}\frac{\partial \boldsymbol{\varepsilon}_m}{\partial T} - \frac{1}{\sigma_m}\frac{\partial \sigma_m}{\partial T}\right)\frac{\boldsymbol{\nabla}T.\boldsymbol{E}}{1+i\omega\tau} \qquad (3)$$

where $i=\sqrt{-1}$, ω is the applied voltage frequency, and $\tau=\frac{\epsilon_m}{\sigma_m}$ is the charge relaxation time.

For aqueous solutions, we can estimate the temperature dependence of the permittivity and conductivity using $\frac{1}{\epsilon_m}\frac{\partial \varepsilon_m}{\partial T}\approx -0.4\%\,°C^{-1}$, and $\frac{1}{\sigma_m}\frac{\partial \sigma_m}{\partial T}\approx -2\%\,°C^{-1}$. The time averaged electrostatic body force is hence given by:

$$\boldsymbol{F}_{ET}=\frac{\boldsymbol{\epsilon}_m}{2}\left(-2.4\%°C^{-1}\frac{\boldsymbol{\nabla}T.\boldsymbol{E}}{1+(\omega\tau)^2}\boldsymbol{E}+0.2\%°C^{-1}|\boldsymbol{E}^2|\boldsymbol{\nabla}\varepsilon_m\right) \quad (4)$$

The fluid flow is described by the time-averaged Stokes equation subject to the electrostatic body force:

$$-\boldsymbol{\nabla}P+\boldsymbol{\nabla}.(\mu_m(T)\boldsymbol{\nabla u})+\boldsymbol{F}_{ET}=\boldsymbol{0} \quad (5)$$

where μ_m is the dynamic viscosity of the fluid, P the pressure, $\boldsymbol{u}$ its velocity.

1.2 Small Temperature Gradient Approximation

In the approximation of small temperature gradients, the changes in fluid properties are also assumed to be small[4]. The electric field is calculated as the sum of the isothermal solution and a small perturbation:

$$\boldsymbol{E}=\boldsymbol{E_0}+\boldsymbol{E_1}, with\ |\boldsymbol{E_1}|\ll|\boldsymbol{E_0}|,\quad \boldsymbol{E_0}=-\boldsymbol{\nabla}V \quad (6)$$

The ACET flow is then estimated by solving the following set of equations:

$$\begin{cases}\nabla^2V=\boldsymbol{0}\\ \boldsymbol{\nabla}.(k_m\,\boldsymbol{\nabla}T)+\frac{\sigma_m}{2}|\boldsymbol{E}|^2=0\\ -\boldsymbol{\nabla}P+\boldsymbol{\nabla}.(\mu_m\boldsymbol{\nabla u})+\boldsymbol{F}_{ET}=\boldsymbol{0}\end{cases} \quad (7)$$

with the corresponding boundary conditions. This system of equation can be solved sequentially since the electrical equation is not coupled with the thermal equation.

The maximum temperature rise can be estimated by $\Delta T\sim\frac{\sigma_m\boldsymbol{V^2}}{k}$ and the ACET fluid velocity is proportional to V^4.

1.3 Model For High Temperature Gradient

At high conductivity, and high voltage, the Joule heating in the fluid is significant which leads to an inaccurate modeling of the AC electrothermal fluid flow by the small temperature gradient approximation.

The electrical field needs to be modeled using the equation:

$$\boldsymbol{\nabla E}=-\frac{\boldsymbol{\nabla}\sigma_m+i\omega\boldsymbol{\nabla}\epsilon_m}{\sigma_m+i\omega\epsilon_m}\boldsymbol{E} \quad (8)$$

The equations for the real and imaginary parts of $\boldsymbol{E}=\boldsymbol{E}_R+i\boldsymbol{E}_I$ are then given by:

$$\boldsymbol{\nabla}\begin{pmatrix}\boldsymbol{E}_R\\ \boldsymbol{E_I}\end{pmatrix}=-R\begin{bmatrix}a & -b\\ b & a\end{bmatrix}\boldsymbol{\nabla}T.\begin{pmatrix}\boldsymbol{E}_R\\ \boldsymbol{E}_I\end{pmatrix} \quad (9)$$

where $R=\frac{1}{1+\omega^2\tau^2}$, $a=\frac{1}{\sigma_m}\frac{\partial\sigma_m}{\partial T}+\omega^2\tau^2\frac{1}{\epsilon_m}\frac{\partial\varepsilon_m}{\partial T}$ and $b=\left(\frac{1}{\epsilon_m}\frac{\partial\varepsilon_m}{\partial T}-\frac{1}{\sigma_m}\frac{\partial\sigma_m}{\partial T}\right)\omega\tau$.

If the $\omega\tau\ll 1$, and the applied voltage on the electrodes has no phase, the equations can be reduced to:

$$\boldsymbol{\nabla E}_R=-\frac{1}{\sigma_m}\frac{\partial\sigma_m}{\partial T}\boldsymbol{\nabla}T.\boldsymbol{E}_R,\quad \boldsymbol{E}_I=0 \quad (10)$$

In terms of electrical potential ($\boldsymbol{E}=-\boldsymbol{\nabla}V$), the equation (10) becomes:

$$\nabla^2V=-\frac{1}{\sigma_m}\frac{\partial\sigma_m}{\partial T}\nabla T.\nabla V \quad (11)$$

The electrical potential is solution of a convection-diffusion equation with convection vector $\boldsymbol{\beta}=-\frac{1}{\sigma_m}\frac{\partial\sigma_m}{\partial T}\nabla T$ and diffusion coefficient D=1.

When there is a high temperature gradient in the fluid, the temperature dependences of the fluid properties cannot be neglected. Hence, the model for AC electrothermal flows is hence given by the following set of equations:

$$\begin{cases}\nabla^2V=-\frac{1}{\sigma_m}\frac{\partial\sigma_m}{\partial T}\nabla T.\nabla V\\ \boldsymbol{\nabla}.(k_m(T)\boldsymbol{\nabla}T)+\frac{\sigma_m}{2}|\boldsymbol{E}|^2=0\\ -\boldsymbol{\nabla}P+\boldsymbol{\nabla}.(\mu_m(T)\boldsymbol{\nabla u})+\boldsymbol{F}_{ET}=\boldsymbol{0}\end{cases} \quad (12)$$

with the appropriate boundary conditions.

2. Experimental Details

Experiments are performed in a 250µm deep PDMS well. Beneath the microwell, three 35µm thick gold electrodes separated by 100µm, deposited on a FR4 board (PCB board), generate an AC electric field. The central 100µm wide electrode is grounded, while a sinusoidal voltage of 1MHz from 0 to 40Vpp is applied to the side electrodes. The microfluidic chamber is covered by a 150µm thick coverlid. The temperature is set under the PCB board at 25°C via a thermoelectric device; the room temperature is set at 23°C. The horizontal section of the flows is measured by PIV 230µm above the gaps.

3. COMSOL Multiphysics Implementation

The AC electrothermal fluid flow is modeled and simulated on COMSOL Multiphysics software. We discuss here the simulation methodology in the context described in paragraph 1.3. The simulation is setup using a 2D stationary solver. The geometry, materials, equations and boundary conditions are presented in Figure 1.

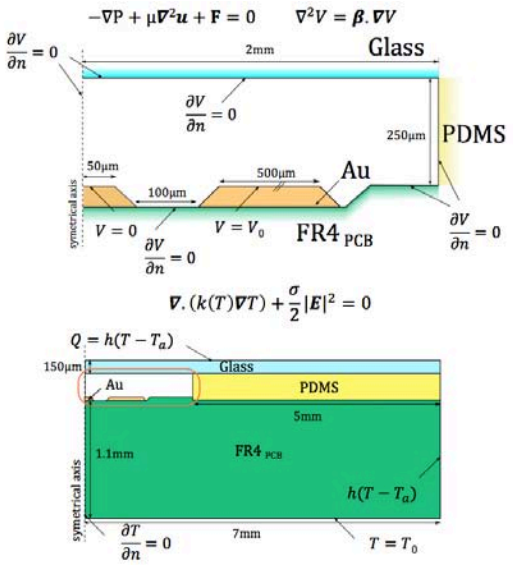

Figure 1. Schematic of the geometrical domain implemented in COMSOL Multiphysics. The geometry details, materials, equations and boundary conditions are summarized.

The electric field equation is calculated using a coefficient form PDE Physic, the thermal equation using a Heat transfer Physic and the fluid flow using a Laminar Flow Physic.

The constant material properties are described in Table 1. The fluid heat conductivity, density and dynamic viscosity are set up using the built in temperature dependent water material properties functions.

Table 1: List of parameters

Parameter	Value
Permittivity of air	8.854188e-12[F/m]
Relative Permittivity of water	80.2
Applied frequency	2 π 1 [MHz]
Conductivity of fluid	8.41, and 0.25 [mS/cm] at 20°C
In-plane heat conductivity of PCB	10 [W/(m K)]
Through heat conductivity of PCB	0.32 [W/(m K)]
Heat conductivity of glass	0.96 [W/(m K)]
Heat conductivity of PDMS	0.15 [W/(m K)]

The fluid electrical conductivity is set up as a variable that depends linearly on the simulated temperature.

The model is solved using a three step strategy. First the pde equation is solved assuming the temperature field is at the initial value (step 1). Then the pde equation is solved coupled with the heat transfer using the solution of step 1 for the pde equation as initial value (step 2). Finally the laminar flow is solved using the solution of step 2 for the dependent variables (step 3). Initial attempts to solve the model without step 1 resulted in non-convergence. The coupling in step 2 is too complex to be solved without an accurate initial value for the pde system.

A parametric simulation is run for values of Vpp between 10 and 40 for two different conductivity values (σ=8.41, and 0.25 mS/cm at 20°C). The assumption $\omega\tau \ll 1$ is justified in these two cases.

4. Results

For the aqueous solution with σ=8.41mS/cm at 20°C, several 2D surface plots are presented. First the contour plot of the electrical potential superimposed with normalized arrow surface of the beta field at Vpp=1V and Vpp=31V are displayed in figure 2 and 3. At high applied voltage, the electrical potential contours move along the beta field toward the center electrode.

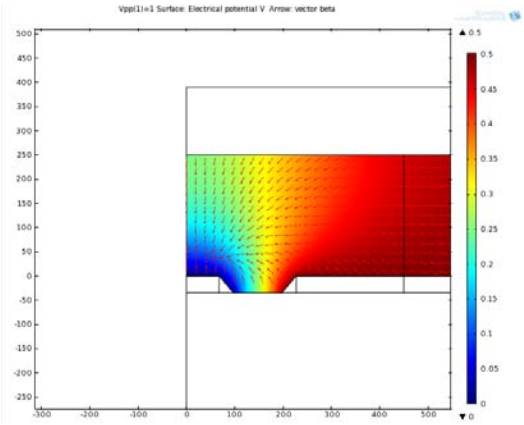

Figure 2. Surface plot of the electrical potential *V*, and normalized arrow surface of the vector $\boldsymbol{\beta} = -\frac{1}{\sigma_m}\frac{\partial \sigma_m}{\partial T}\nabla T$ for aqueous solution with *σ=8.41mS/cm at 20°C* and *Vpp=1V*.

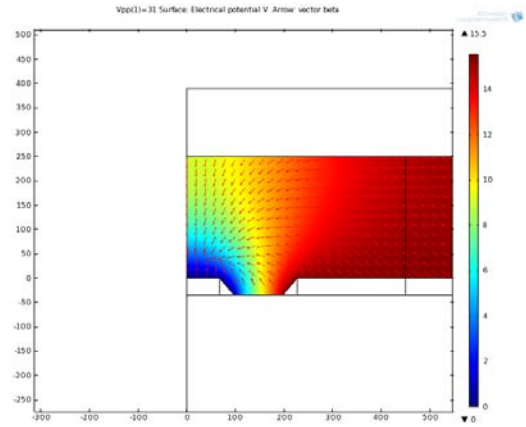

Figure 3. Surface plot of the electrical potential V, and normalized arrow surface of the vector $\boldsymbol{\beta} = -\frac{1}{\sigma_m}\frac{\partial \sigma_m}{\partial T}\nabla T$ for aqueous solution with σ=8.41mS/cm at 20°C and Vpp=31V.

Contour plots of the temperature field is extracted for value of Vpp=19V (see Figure 4). The maximum temperature in that case is 362.72K. Experiments for higher applied voltage showed the appearance of bubbles which may correspond to high temperature in the fluid (see Figure 5).

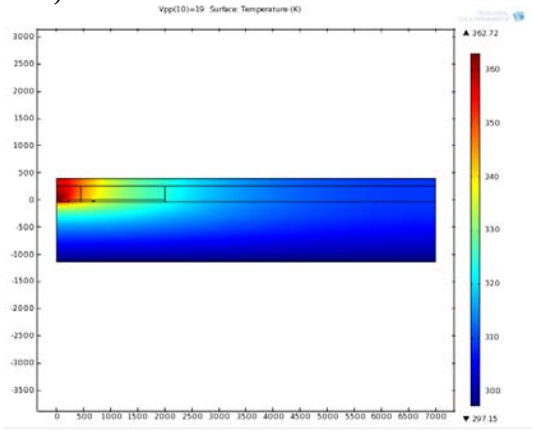

Figure 4. Surface plot of the temperature for aqueous solution with σ=8.41mS/cm at 20°C and Vpp=19V.

For the two different conductivity values, the applied voltage dependence of the velocity in the x-direction at x=190µm, y=200µm from the COMSOL simulations are compared to the experimental measures (Figure 5 and 6).

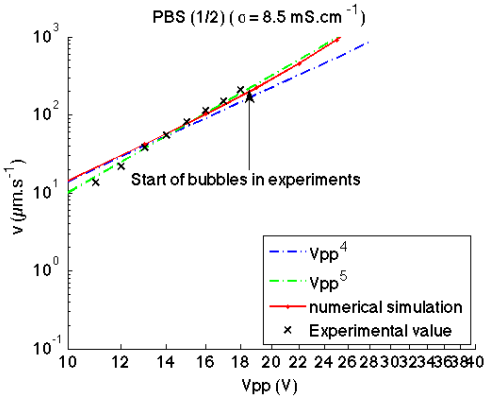

Figure 5. Dependence of the ACET velocity to the applied Vpp voltage at σ=8.41mS/cm at 20°C. COMSOL simulation results (red) are compared to experimental values (cross).

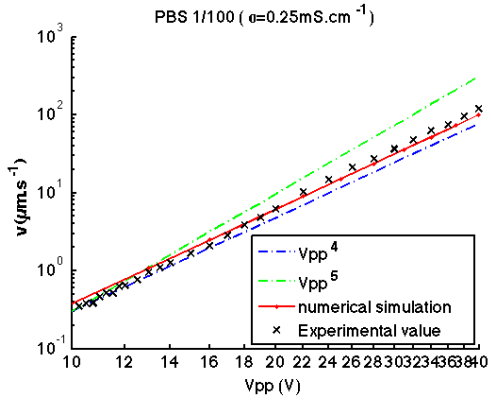

Figure 6. Dependence of the ACET velocity to the applied Vpp voltage at σ=0.25mS/cm at 20°C. COMSOL simulation results (red) are compared to experimental values (cross).

At low conductivity, velocity flow does follow V^4 whereas at higher conductivities where joule heating is more significant the flows velocities tend to fit V^5.

7. Conclusions

Results of numerical simulations are presented and compared with experiments. Our fully electro-thermal coupled theory successfully fit the experimental flows for high temperature gradient. The set of equations is solved using COMSOL Multiphysics, which allows to solve the strong coupling between electrical and heat equations successfully.

8. References

[1] A. Castellanos, A. Ramos, A. Gonzales, N. G. Green, and H. Morgan, Electrohydrodynamics and dielectrophoresis in microsystems: scaling law, *Journal of Physics D: Applied Physics*, **vol. 36**, pp. 2584–2597 (2003).

[2] M F M Speetjens et al, Multi-functional Lagrangian flow structures in three-dimensional ac electro-osmotic micro-flows, *Fluid Dynamics Research*, **vol. 43**(3), p. 035503 (2011).

[3] M. L. Y. Sin, V. Gau, J. C. Liao, and P. K. Wong, Electrothermal Fluid Manipulation of High-Conductivity Samples for Laboratory Automation Applications, *Journal of the Association for Laboratory Automation*, **vol. 15**(6), pp. 426-432 (2010).

[4] A. Ramos, H. Morgan, N. G. Green, and A. Castellanos, AC Electric-Field-Induced Fluid Flow in Microelectrodes, *Journal of Colloid and Interface Science*, **vol. 217**(2), pp. 420-422 (1999).